

Shrinkage properties of ceramic injection moulding part with a step-contracted cross-section in the filling direction

Ren-Haw Chen*, Chi-Hung Ho, Hong-Chang Fan

Department of Mechanical Engineering, National Chiao Tung University, 1001 Ta Hsueh Road, 30010 Hsinchu, Taiwan, ROC

Received 1 September 2003; received in revised form 20 September 2003; accepted 28 October 2003

Available online 19 March 2004

Abstract

The need for ceramic materials in microelectromechanical systems (MEMS) is increasing quickly. A typical form of designed ceramic micro parts involves the structuring of several micro columns and/or thin walls on a substrate. This work considers the use of a model mould with a straight mould cavity and a step-contracted cross-section in the filling direction. The injection moulding of such of ceramic micro part is experimentally simulated. The effect of the mould cavity contraction ratio, moulding conditions, and the solid loading of the ceramic/binder mixture on the distribution of the transverse shrinkage of the moulding parts at moulded, debinded, and sintered stages, respectively, are examined. Experimental results reveal that transverse shrinkage of the region downstream from the step-contracted cross-section clearly exceeds that of the region upstream in all three stages. Furthermore, transverse shrinkage varies greatly in the plane of the step-contracted cross-section. The magnitude of the variation in transverse shrinkage in the step-contracted cross-section increases with the contraction ratio of the mould cavity. Appropriately increasing either the holding pressure or the filling pressure of the mould cavity reduces the variation in the transverse shrinkage of the step-contracted cross-section. Moreover, using the ceramic/binder mixture with a composition similar to that of critical solid loading can lower the internal stress caused by sintering in the vicinity of the step-contracted cross-section.

© 2004 Elsevier Ltd and Techna Group S.r.l. All rights reserved.

Keywords: A. Injection moulding; Micro parts; Shrinkage

1. Introduction

Microelectromechanical systems (MEMS), actively developed in recent years, have increased the demand for ceramic materials [1–4]. Normally, the designed ceramic micro part includes micro columns and/or thin walls built upwardly from a ceramic substrate [1–3,5,6]. The injection moulding of ceramic micro parts with such forms raises the following two main problems. (1) Micro-structures (columns, walls, and others), especially those with higher aspect ratios, crack and collapse from the foundations connected to the substrate, which may occur after moulding, debinding or sintering. (2) The lateral dimensions (including diameter, width, thickness) of fabricated micro-structures are difficult to control, raising difficulties in designing mould inserts [7–9]. One of the primary causes of these problems is thought to be the unique material flow and shrinkage properties due to the injection moulding of products with the form described above [7]. Hence, accurately

elucidating the characteristics, with reference to moulding, of the form of the micro parts and then investigating the associated fundamental shrinkage properties are essential.

The mould cavity used to fabricate ceramic micro parts with the aforementioned form can be broadly divided into two parts—the sub-cavity that allow the substrate to be formed and all the other sub-cavities that enable the micro-structures to be generated on the substrate. Generally, the moulding material fills the former part from the gate and then flows into the latter part during the filling stage of the injection moulding. Moreover, the cross-sectional area, through which the moulding material can flow, of the former part always far exceeds that of the latter part, in a practical mould cavity, regardless of the location of the gate. Consequently, the moulding material undergoes step-contraction in the flow channel, while the micro-structures of a micro part are being formed. The step-contraction due to flow channel is inevitable in micro injection moulding.

In this study, model mould cavities, with step-contracted cross-sections in the filling direction, for ceramic micro injection moulding, are designed, as depicted in Fig. 1. The wide part, to which the gate attached, represents the

* Corresponding author. Fax: +886-3-572-0634.

E-mail address: chenrh@mail.nctu.edu.tw (R.-H. Chen).

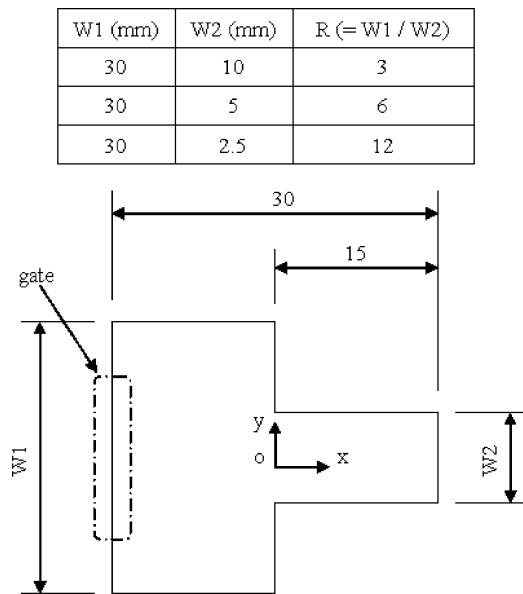


Fig. 1. Cavity dimensions of the mould inserts used in the experiments. All the mould cavities are made with a uniform depth of 3 mm. R is the contraction ratio of the cross-sectional area at $x = 0$.

sub-cavity for forming the substrate and the narrow part, which is far from the gate, represents the sub-cavity for creating a single micro-structure. Using the model mould cavities, ceramic injection moulding experiments are performed to simulate the filling of the cavity during the injection moulding of the ceramic micro parts. The variations in width in the filling direction of the moulded, debinded, and sintered bodies, respectively are plotted and compared with the corresponding dimensions of the model mould cavity, to elucidate the transverse shrinkage of the working part in each stage of the injection moulding process.

2. Experimental procedure

Polymeric binder was kneaded with alumina powder (Model AL-45-1, Showa Denko K.K., Tokyo, Japan) with a solid loading of 57, 61, 63 and 65%, for 3 h, to prepare the material used in injection moulding experiments. The polymeric binder includes low-density polyethylene (LDPE) (USI Far East Co., Taipei, Taiwan), paraffin wax (PW) (Showa Chemicals, Tokyo, Japan), and stearic acid (SA) (Showa Chemicals, Tokyo, Japan). Tables 1 and 2 show the powder characteristics and the compositions of experi-

Table 1
Characteristics of the alumina powder used^a

Model	Specific gravity	Mean particle size (μm)	Bulk density (g cm^{-3})		BET specific surface area ($\text{m}^2 \text{g}^{-1}$)
			Loosed	Tapped	
AL-45-1	3.94	1.8	0.8	1.4	1.8

^a From product specification of Showa Denko, Ltd.

Table 2
Compositions of the experimental materials (vol.%)

Code	Alumina	Binder		
		LDPE ^a	Paraffin wax ^b	Stearic acid ^c
A	57.0	10.8	30.1	2.1
B	61.0	9.8	27.3	1.9
C	63.0	9.3	25.9	1.8
D	65.0	8.8	24.5	1.7

^a From product specifications of USI Far East Co. ($\rho = 0.91 \text{ g cm}^{-3}$, melting temperature 115°C).

^b From product specifications of Showa Chemicals ($\rho = 0.92 \text{ g cm}^{-3}$, melting temperature $60\text{--}63^\circ\text{C}$).

^c From product specifications of Showa Chemicals ($\rho = 0.94 \text{ g cm}^{-3}$, melting temperature $68\text{--}71^\circ\text{C}$).

Table 3
Conditions of the injection moulding experiments

Parameter	Values
Mould temperature ($^\circ\text{C}$)	40, 50, 60, 70
Barrel temperature ($^\circ\text{C}$)	130, 150, 160, 170
Injection pressure (MPa)	26.6
Injection plunger velocity (mm s^{-1})	33, 50, 100
Holding pressure (MPa)	15.9, 21.3, 26.6
Holding time (s)	0, 6

mental materials, respectively. The critical solid loading of materials in this work is 63 vol.%. The green pellets, just before moulding, were dried at 50°C for 12 h to remove the moisture.

A plunger type injection-moulding machine (Shinko Sellbic Co., Tokyo, Japan) is used to pack the experimental material into the mould cavity that is illustrated in Fig. 1. Table 3 summarise the experimental conditions used in this study. After moulding, the widths at various positions along the filling direction of each moulded green part were measured using a CCD microscope (Model CV-950, JAI Corp., Kanagawa, Japan) which was with a stage with an x - y positioning resolution of $1 \mu\text{m}$.

Here, solvent debinding was conducted. The moulded green parts were immersed in gasoline, which was used as a solvent, at 25°C for 72 h to remove almost all of the binder in the moulded green parts, excluding the LDPE. Then, sintering was performed in an electric furnace (Model HT-16/17, Nabertherm GmbH, Lilienthal, Germany) up to 1600°C . Also, the widths of both the debinded parts and the sintered parts were measured after debinding and sintering, respectively.

3. Results and discussion

Transverse shrinkages of the moulded parts in the filling direction are calculated from measured width data of the model mould cavities and the moulded parts. Fig. 2 shows a typical distribution of transverse shrinkage in the filling direction, of a ceramic injection moulded green part with

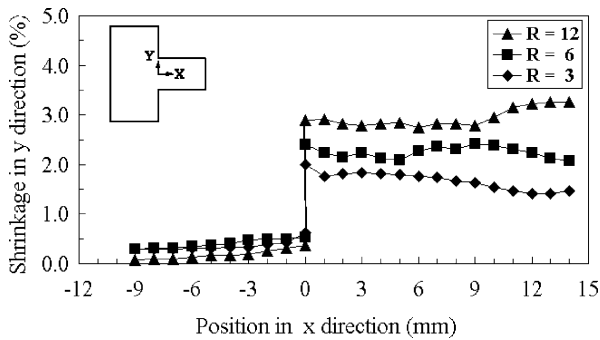


Fig. 2. Transverse shrinkage variations, measured in the material filling direction, of the moulded green parts when the mould insert, that includes a cavity, as illustrated in Fig. 1, was used for the injection moulding (R : contraction ratio). Mould temperature 60°C , barrel temperature 150°C , injection plunger velocity 50 mm s^{-1} and solid loading 61 vol.%.

a step-contracted section. The amount of the transverse shrinkage in the region upstream from the step-contracted section clearly differs from that in the region downstream: the former is smaller and the latter is larger, resulting in an acute variation in the transverse shrinkage of the step-contracted section. The variation of transverse shrinkage in the step-contracted section tends to increase with the contraction ratio, R . These results imply that the linear density of the binders in the transverse direction downstream from the step-contracted section of the green part exceeds that upstream since the shrinkage of the ceramic green part results mainly from the cooling and solidifying shrinkage of binders in the moulding material [10], probably for the following reasons. (1) The moulding material suffers a very large shear action as it flows through the step-contracted section, and the sudden increase in shear stress causes the particles of ceramic powder to be oriented in the direction of shear. (2) The sudden increase in shear stress causes the packing of the ceramic powder in the moulding material to change from close to loose as the material flows through the step-contracted section, causing “binder absorbing” like that of dilatant fluid [11,12]. (3) Both of these effects occur. The conditions of transverse shrinkage variation in the filling direction are critical in designing a mould insert and controlling the dimensions and the shape of the final ceramic products. In particular, the rapid variation in transverse shrinkage in the step-contracted section widely distributes internal stress in the material near the step-contracted section, often causing cracking at the connection between the wide and the narrow parts.

Fig. 3 shows the effect of the contraction ratio on the difference between the transverse shrinkage of the wide and that of the narrow side of the step-contracted section at various injection plunger speeds. Typically, the difference between the transverse shrinkage of each side of the step-contracted section increases with the contraction ratio. However, its rate of increase declines as the contraction ratio increases, because the amount of material that flows through the step-contracted section is finite and the shear action suf-

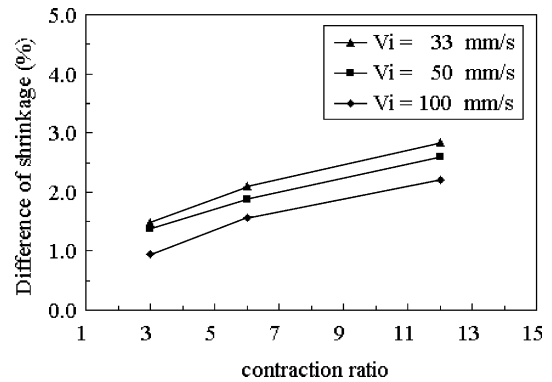


Fig. 3. Effect of contraction ratio on the difference in transverse shrinkage measured at the step-contracted section ($x = 0$) for various injection plunger velocities (V_i : injection plunger velocity). Mould temperature 60°C , barrel temperature 150°C and solid loading 61 vol.%.

fices to cause most of the material that passes through this section to exhibit the behaviours described as (1)–(3) before, when the contraction ratio increases to a relatively high value. Notably, for a fixed contraction ratio, the difference between the transverse shrinkages in the step-contracted section decreases as the speed of the injection plunger increases. This result implies that the material undergoes less shearing and more pressure-packing as the injection plunger speed is increased, although a higher injection speed increases both the shear on the material that flows through the contracting section and the pressure in the cavity.

Fig. 4 presents the effect of barrel temperature (material temperature) on the difference in the transverse shrinkage in the step-contracted section. As the temperature of the moulding material increases, the difference in the shrinkage in the step-contracted section increases only slightly. Clearly, increasing the temperature of the material does not impact the mechanism of shrinkage of the ceramic green parts which have a step-contracted cross-section in the filling direction.

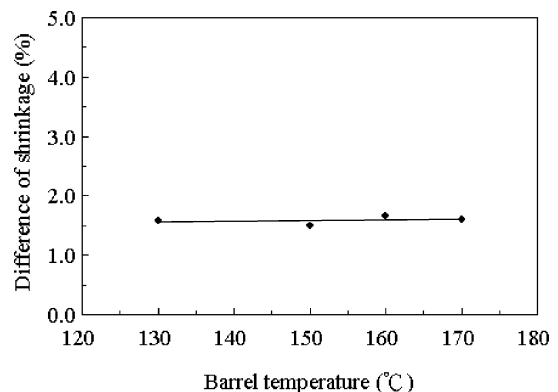


Fig. 4. Effect of barrel temperature on the difference in transverse shrinkage measured at the step-contracted section ($x = 0$) following moulding. The line represents the trend in the experimental data. Cavity contraction ratio 6, mould temperature 60°C , injection plunger velocity 100 mm s^{-1} , solid loading 61 vol.%.

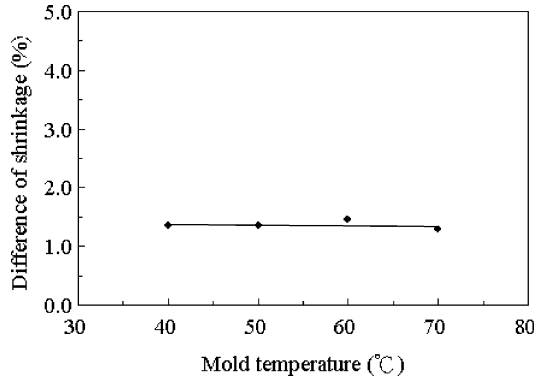


Fig. 5. Effect of mould temperature on the difference in transverse shrinkage measured at the step-contracted section ($x = 0$) following moulding. The line represents the trend in the experimental data. Cavity contraction ratio 6, barrel temperature 150 °C, injection plunger velocity 100 mm s⁻¹, solid loading 61 vol.%.

In ceramic injection moulding, the set mould temperature affects the rate at which the mould cools the moulding material, which strongly influences the flow of the material in the filling stage. Fig. 5 shows the effect of mould temperature on the difference in transverse shrinkage in the step-contracted section. Although the highest mould temperature in this work exceeds the melting temperatures of the binders PW and SA that are contained in the material, the experimental result shows that the mould temperature does not impact the difference in transverse shrinkage in the step-contracted section.

Fig. 6 presents the effect of holding pressure on the difference in transverse shrinkage in the step-contracted section. Clearly, an appropriate holding pressure reduces the difference in transverse shrinkage in the step-contracted section, because increasing the holding pressure reduced the transverse shrinkage downstream from the step-contracted section more than that upstream. Reducing the difference in transverse shrinkage in the step-contracted section by increasing the holding pressure is one effective means of

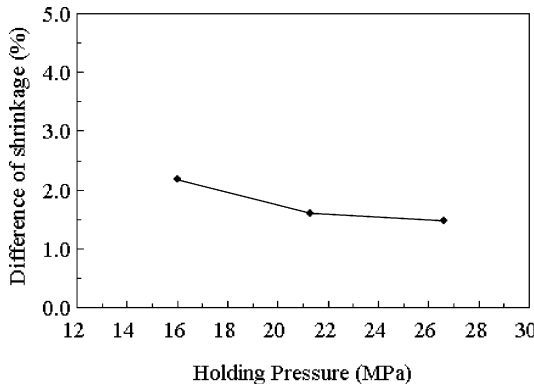


Fig. 6. Effect of holding pressure on the difference in transverse shrinkage measured at the step-contracted section ($x = 0$) after moulding. Cavity contraction 6, mould temperature 60 °C, barrel temperature 150 °C, injection plunger velocity 100 mm s⁻¹, solid loading 61 vol.%.

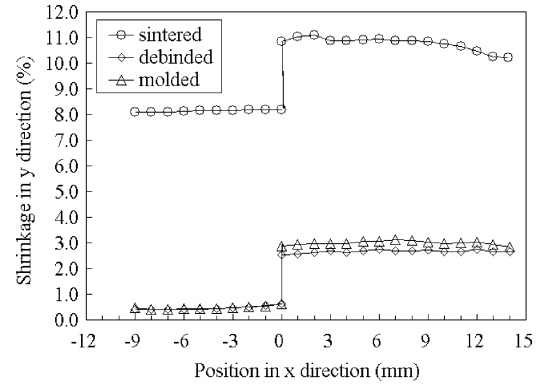


Fig. 7. Variations in transverse shrinkage in the material filling direction in a ceramic part, measured following moulding, debinding, and sintering, respectively. This part is injection moulded using a mould insert with a cavity, as shown in Fig. 1. Cavity contraction ratio 6, mould temperature 60 °C, barrel temperature 150 °C, injection plunger velocity 100 mm s⁻¹, solid loading 61 vol.%.

reducing the probability of generating defects during moulding and later processes. However, this method does not completely eliminate the difference in transverse shrinkage that results from the step-contraction of the flow channel in the mould. Notably, excessive holding pressure causes un-solidified liquid binders to seep out, causing further problems.

The moulded ceramic green part must still be debinded and sintered into the final product. Fig. 7 displays the variation in transverse shrinkage, measured in the filling direction after the moulding, debinding and sintering, of ceramic injection moulding parts that include a step-contracted section. Clearly, the transverse shrinkage measured after debinding is smaller than that measured after moulding in the region downstream from the step-contracted section, slightly reducing the difference in transverse shrinkage in the step-contracted section to about 83% of that obtained after moulding. The swelling of moulded ceramic green part after debinding is considered to be due to residual LDPE, which is one of the constituents of the binders, and is insoluble in the debinding solvent [13]. However, the transverse shrinkage in all positions in the filling direction is greatly increased by sintering. In particular, the increasing range in the transverse shrinkage downstream from the step-contracted section exceeds that upstream, increasing the difference in transverse shrinkage in the step-contracted section to approximately 37% over that obtained after debinding. The decrease and increase in the difference in transverse shrinkage in the step-contracted section during debinding and sintering, respectively, are such that the stress field near the step-contracted section must be varying at that time. The variation in stress may increase the probability of warping and cracking.

Fig. 8 plots the effect of the solid loading of the moulding material on the difference in the transverse shrinkage in the step-contracted section. For the moulded green parts, the difference in the transverse shrinkage reaches a maximum when a material with a composition close to that of

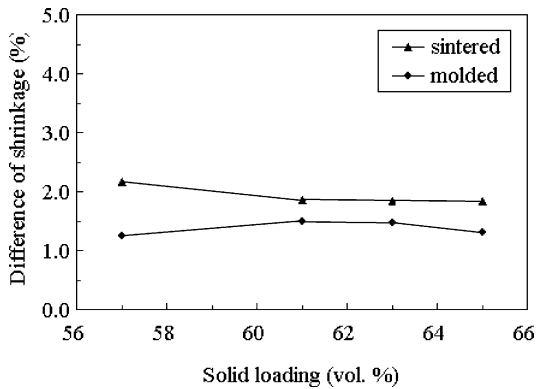


Fig. 8. Effect of the solid loading of the moulding material on the difference in transverse shrinkage measured at the step-contracted section ($x = 0$) following moulding and sintering. Cavity contraction 6, mould temperature 60 °C, barrel temperature 150 °C, injection plunger velocity 100 mm s⁻¹.

the critical solid loading is used. Such a result is considered to follow from the two following reasons. (1) A higher solid loading implies that more powders are orientated and their packing states altered to loosen them, due to the shear action during flow through the step-contracted section. Therefore, the potential for the material to shrink downstream from the step-contracted section is increased. (2) The material with a composition that exceeds the critical solid loading includes poor binders, producing shrinkage. However, for the sintered parts, a lower solid loading is associated with a larger difference in the transverse shrinkage. Thus, as depicted in Fig. 8, using the material with a composition close to the critical solid loading can cause the increase in the difference in transverse shrinkage in the step-contraction section during sintering to be minimal.

4. Conclusions

The step-contraction of the material flow channel is characteristic of the injection moulding of ceramic parts with micro-structures that are attached to the substrates. This characteristic significantly affects the flow behaviour of the powder/binder mixed moulding material during the filling stage. The direct consequences affect the uniformity of the distribution of the transverse shrinkage, the accuracy of the dimensions, the shape of the final products, and the probability of generating defects. This paper investigated the shrinkage properties of the products of such ceramic injection moulding with a step-contracted section in the filling direction. The main conclusions are as follows.

- (1) The step-contracted section increases the downstream transverse shrinkage more than that upstream, after moulding, debinding, or sintering, resulting in a severe variation in transverse shrinkage in the step-contracted section. This extreme variation in transverse shrinkage in the step-contracted section is

a potential cause of the collapse of micro-structures from the substrate.

- (2) A smaller contraction ratio, a higher injection plunger speed (increasing the internal pressure within the mould cavity in filling), and a higher holding pressure promote the decrease in the variation in transverse shrinkage in the step-contracted section.
- (3) The difference between the transverse shrinkage downstream and that upstream of the step-contracted section increases during sintering.
- (4) Although using a material with a composition similar to the critical solid loading increases the difference in the transverse shrinkage in the step-contracted section after moulding. However, using such a material minimises the enlargement of the difference of transverse shrinkage during sintering, reducing the sintering stress and the probability of the formation of defects.

Acknowledgements

The authors would like to thank Professor S.Y. Chen of the Department of Materials Science and Engineering, NCTU for his many valuable comments and suggestions.

References

- [1] R. Knitter, D. Göhring, P. Risthaus, J. Haußelt, Microfabrication of ceramic microreactors, *Microsyst. Technol.* 7 (2001) 85–90.
- [2] V. Piotter, W. Bauer, T. Benzler, A. Emde, Injection molding of components for microsystems, *Microsyst. Technol.* 7 (2001) 99–102.
- [3] H. Freimuth, V. Hessel, H. Kölle, M. Lacher, W. Ehrfeld, Formation of complex ceramic miniaturized structures by pyrolysis of poly(vinylsilazane), *J. Am. Ceram. Soc.* 79 (6) (1996) 1457–1465.
- [4] C. Harris, M. Despa, K. Kelly, Design and fabrication of a cross flow micro heat exchanger, *J. Microelectromech. Syst.* 9 (4) (2000) 502–508.
- [5] L.J. Bowen, K.W. French, Fabrication of piezoelectric ceramic/polymer composites by injection molding, in: *Proceedings of the Eighth IEEE International Symposium in Applications of Ferroelectrics*, 1992, pp. 160–163.
- [6] R.H. Chen, C.L. Lan, Fabrication of high-aspect-ratio ceramic microstructures by injection molding with the altered lost mold technique, *J. Microelectromech. Syst.* 10 (1) (2001) 62–68.
- [7] A. Safari, V. Janas, R. Panda, Fabrication of fine-scale 1-3 pb(zrx, Ti_{1-x})O₃ ceramic/polymer composites using a modified lost mold method, in: *Proceedings of SPIE Smart Structures and Materials 1996 in Industrial and Commercial Applications of Smart Structures Technologies*, 1996, pp. 251–262.
- [8] R.M. German, Molding tooling and equipment/tooling, in: *Polymer Injection Molding*, Metal Powder Industries Federation, Princeton, NJ, 1990, pp. 249–260.
- [9] R. Billiet, The challenge of tolerance in P/M injection molding, in: H.I. Sanderow, W.L. Giebelhausen, K.M. Kulkarni (Eds.), *Progress in Powder Metallurgy*, vol. 41, Metal Powder Industries Federation, Princeton, NJ, 1985, pp. 723–741.
- [10] S. Iwahashi, Mold technology for powder injection molding, *Plastics* 40 (5) (1994) 53–58 (in Japanese).

- [11] R.I. Tanner, Introduction to rheology/description of non-Newtonian fluid behaviour in shear, in: *Engineering Rheology*, Oxford University Press, New York, 1988, pp. 11–16.
- [12] J.L. White, Experimental observations of rheological behavior of polymer systems/development of rheological concepts, in: *Principles of Polymer Engineering Rheology*, John Wiley & Sons, Inc., New York, 1990, pp. 138–140.
- [13] K. Ono, Y. Kaneko, Y. Kankawa, K. Saitou, N. Kasahara, Injection molding of silicon nitride with solvent debinding, *Powder Powder Metall.* 39 (8) (1992) 690–694 (in Japanese).